The effect of nanoparticle softness on the interfacial dynamics of a model polymer nanocomposite

Zhu, Yuwen; Giuntoli, Andrea; Zhang, Wengang; Lin, Zhongqin; Keten, Sinan; Starr, Francis W.; Douglas, Jack F.

[Link to publication in University of Groningen/UMCG research database](#)

The effect of nanoparticle softness on the interfacial dynamics of a model polymer nanocomposite

Yuwen Zhu, Andrea Giuntoli, Wengang Zhang, et al.

ARTICLES YOU MAY BE INTERESTED IN

Understanding the role of cross-link density in the segmental dynamics and elastic
properties of cross-linked thermosets
The Journal of Chemical Physics **157**, 064901 (2022); https://doi.org/10.1063/5.0099322

Confinement free energy for a polymer chain: Corrections to scaling
The Journal of Chemical Physics **157**, 094902 (2022); https://doi.org/10.1063/5.0105142

Relating dynamic free volume to cooperative relaxation in a glass-forming polymer
composite
The Journal of Chemical Physics **157**, 131101 (2022); https://doi.org/10.1063/5.0114902

The effect of nanoparticle softness on the interfacial dynamics of a model polymer nanocomposite

View Online   Export Citation   CrossMark

Yuwen Zhu,[1,2] (iD) Andrea Giuntoli,[3] (iD) Wengang Zhang,[4,5] (iD) Zhongqin Lin,[1,6] Sinan Keten,[2,7,a)] (iD)
Francis W. Starr,[4] (iD) and Jack F. Douglas[5,a)] (iD)

AFFILIATIONS

[1] State Key Laboratory of Mechanical System and Vibration, Shanghai Jiao Tong University, Shanghai 200240,
People's Republic of China
[2] Department of Civil and Environmental Engineering, Northwestern University, 2145 Sheridan Road, Evanston,
Illinois 60208-3109, USA
[3] Zernike Institute for Advanced Materials, University of Groningen, 9747 AG Groningen, The Netherlands
[4] Department of Physics, Wesleyan University, Middletown, Connecticut 06459, USA
[5] Materials Science and Engineering Division, National Institute of Standards and Technology, Gaithersburg,
Maryland 20899, USA
[6] Shanghai Key Laboratory of Digital Manufacture for Thin-walled Structures, Shanghai Jiao Tong University,
Shanghai 200240, People's Republic of China
[7] Department of Mechanical Engineering, Northwestern University, 2145 Sheridan Road, Evanston, Illinois 60208-3109, USA

[a)] Authors to whom correspondence should be addressed: s-keten@northwestern.edu and jack.douglas@nist.gov

ABSTRACT

The introduction of soft organic nanoparticles (NPs) into polymer melts has recently expanded the material design space for polymer nanocomposites, compared to traditional nanocomposites that utilize rigid NPs, such as silica, metallic NPs, and other inorganic NPs. Despite advances in the fabrication and characterization of this new class of materials, the effect of NP stiffness on the polymer structure and dynamics has not been systematically investigated. Here, we use molecular dynamics to investigate the segmental dynamics of the polymer interfacial region of isolated NPs of variable stiffness in a polymer matrix. When the NP–polymer interactions are stronger than the polymer–polymer interactions, we find that the slowing of segmental dynamics in the interfacial region is more pronounced for stiff NPs. In contrast, when the NP–polymer interaction strength is smaller than the matrix interaction, the NP stiffness has relatively little impact on the changes in the polymer interfacial dynamics. We also find that the segmental relaxation time τ_α of segments in the NP interfacial region changes from values lower than to higher than the bulk material when the NP–polymer interaction strength is increased beyond a "critical" strength, reminiscent of a binding–unbinding transition. Both the NP stiffness and the polymer–surface interaction strength can thus greatly influence the relative segmental relaxation and interfacial mobility in comparison to the bulk material.

INTRODUCTION

The addition of nanofillers to a polymer matrix is a growing trend in material science that allows for tuning the macroscopic properties of polymer-based composites by manipulating their nanoscale structure and composition.[1,2] Silica nanoparticles (NPs) are common nanofillers that can improve the mechanical properties of polymer materials, such as Young's modulus and toughness,[3–5] and also lead to the emergence of new features, such as reproducing the optical properties of complex biomaterials, such as the chameleon's skin.[6] The application potential of silica NP filled polymer composites is limitless, ranging from the pharmaceutical,[7,8] aerospace,[9,10] to automotive industries.[11,12] The increased material performance that comes from this widening in the design space

of chemical compositions can be anticipated to arise from a modification of interfacial interactions with the polymer matrix, but the origin of these property changes is not completely understood, since changes in polymer dynamics near the NP interfaces are hard to observe experimentally and anticipate theoretically. Molecular simulations offer opportunities to better understand these property changes, since this approach has the requisite spatial and temporal resolution to study interfacial dynamics. Here, we use this approach to study the effect of nanoparticle rigidity on the *segmental dynamics* in the interfacial region of the composite. Our analysis is restricted to the dilute limit to avoid complications that can arise when the interfacial zones of different particles overlap.

Many previous simulations[13–15] and experimental studies[16–19] have attempted to unravel the molecular mechanisms underlying the performance enhancements sometimes found when adding NPs to polymer matrices, and most of these studies have focused on the addition of stiff, nearly un-deformable NPs in a polymer matrix. The current literature has considered the effects of NP size,[20,21] concentration,[21–23] size dispersity,[24] polydispersity,[21] surface roughness,[22] and NP–polymer interaction.[19] From the perspective of polymer melt structure, for instance, the presence of NPs with repulsive NP–polymer interaction apparently has little impact on local chain conformations, although the radius of gyration of chains increases somewhat in composites having attractive NPs.[25] This leads to a non-linear density gradient from the NP surface to the neat polymer matrix. In addition to local structural changes upon adding NPs, the segmental dynamics in the polymer matrix clearly change around the NPs, where we also observe, as in previous investigations, that there is no direct correlation between the density gradient and the mobility gradient around the NPs.[26,27] In general, a reduced mobility of chain segments near an attractive NP surface is observed.[17] However, the spatial extent of the interfacial mobility layer is modest in comparison to the size of a typical NP, extending to a distance of no more than ≈ 5 nm in amorphous glass-forming polymers.[28] Nonetheless, this layer can sometimes exert a large influence on the properties of nanocomposites.

In practice, it is often difficult to disperse the NPs homogeneously in the polymer matrix, and this has led to a growing interest in using organic "soft" NPs, such as single chain polymer NPs, polymer-grafted NPs, or star polymers, where a judicious choice of the polymer topology and NP–polymer interaction can aid the relatively homogeneous dispersion of the NPs.[29] Besides dispersion, researchers have also started to pay more and more attention to "soft" NPs, such as in the field of soft robotics, where nanoparticles made of liquid metals are used,[30] allowing for the optimization of the viscosity of NP/polymer mixtures under processing conditions,[31,32] the plateau modulus when the polymer matrix is entangled,[31] and both the rate of polymer and NP diffusion in the nanocomposite.[33–37] With the addition of soft NPs, the viscosity and the plateau modulus both tend to decrease with increasing NP concentration, accompanied by an intriguing breakdown of the Stokes–Einstein equation relating the rate of diffusion to the fluid viscosity.[32] The incorporation of spherical NPs with a radius $R \approx 10$ nm has been shown to increase the rate of diffusion of polymer chains (radius of gyration, $R_g \approx 20$ nm) in the melt.[33] More generally, this type of change is controlled by the relative size of the NPs to the polymer chains.[38] However, there are

significant complexities and the measurement of segmental dynamics in the interfacial region is inherently difficult.[21,39,40] The mechanism behind the effect of soft NPs on the polymer dynamics is particularly poorly understood.

In the present work, we perform coarse-grained molecular dynamics (CG-MD) simulations of a single NP in a polymer matrix, where we tune both the softness of the NP at varying temperature and NP–polymer interaction strength. Slower polymer segmental interfacial dynamics are observed with a strongly attractive NP–polymer interaction, consistent with many prior studies.[26,27] We show that the magnitude of this effect can be enhanced by increasing NP stiffness. A crossover is observed for threshold values of the NP stiffness and NP–polymer interaction strengths where the segmental dynamics compared to the pure polymer matrix changes from being faster to slower. This provides insights into the molecular origin of the structural and dynamical changes induced by adding soft NPs to polymer matrices that should be useful in the design of composite materials. Thus, while the density gradient cannot by itself predict the mobility gradient around NPs, changes in the interfacial mobility can signal changes in the interfacial density profile, possibly signaling the occurrence of molecular binding to the polymer matrix. The change in the density profile near the substrate is apparent in the case of polymer films supported on solid substrates.[41] However, the observation of this type of density "anomaly," defined by a change in the sign of the derivative of the density near the solid interface, can be obscured in the case of non-spherical particles, and this complication is more pronounced in the case of the very soft particles studied here, which can spontaneously adopt deformed shapes.

RESULTS AND DISCUSSION

Effect of nanoparticle stiffness on mobility interfacial zone

Since our main goal is to quantify the effect on the polymer segmental dynamics in the NP–polymer interfacial region when the stiffness of the nanoparticle is changed, along with other parameters, such as temperature and NP–polymer interaction strength (which are quantities investigated in our previous work[26,27]), we focus on the limit of isolated NPs where the interfacial layers of different NPs do not interact. In our coarse-grained polymer model, NP stiffness is specified by a stiffness parameter k, defined by a harmonic potential of the bonds tethering the NP beads to their original location (see Fig. 1 and the "Methods" section for details).

We evaluate the self-intermediate scattering function $F_s(q,t)$ and the relaxation time τ_α as a function of the distance r from the NP surface, as described in the Methods section. Figures 1(a) and 1(b) show the simulation setup, visualizing the segmental relaxation time in the vicinity of the NP for a weakly attractive NP–polymer interaction strength ($\varepsilon_{NP-P} = 0.1$) and a strongly attractive NP–polymer interaction strength ($\varepsilon_{NP-P} = 1.5$), respectively. Figures 2(a) and 2(b) show the variation of $F_s(q,t)$ approaching the NP surface for weakly and strongly attractive NP–polymer interaction strength at a fixed T and k. The segmental interfacial dynamics is evidently slowed by a strong NP–polymer interaction, while it is accelerated by a weak NP–polymer interaction strength, as discussed previously for "hard" NPs[26,27] and for the segmental dynamics in the
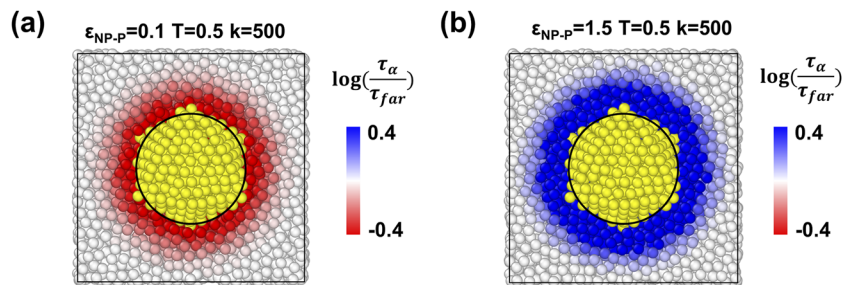
FIG. 1. Visualization of the gradient of relaxation time τ_α around the NP at stiffness $k = 500$ and temperature $T = 0.5$ for systems having either (a) weakly $\varepsilon_{NP-P} = 0.1$ or (b) strongly $\varepsilon_{NP-P} = 1.5$ attractive interaction, compared to the pure polymer relaxation time τ_{far}. The interfacial polymer dynamics speed up with weak interaction, while they are slowed down with strong attractive interaction. The NP beads are colored in yellow.

substrate interfacial region of supported polymer films.[42–44] From $F_s(q,t)$, we can quantify the relaxation time $\tau_\alpha(r)$, as described in "Methods" section. Figures 2(c) and 2(d) present the distance r dependence of the relative relaxation time $\tau_\alpha(r)/\tau_{far}$ with varying k and T, respectively, where τ_{far} is the value of the relaxation time in the bulk, far away from the NP surface. For an infinitely dilute system, τ_{far} only depends on the temperature T and must correspond to the segmental relaxation time of the bulk material. In our simulations, we observe a relatively small deviation of τ_{far} from the bulk limit estimate that depends on the strength of ε_{NP-P}, but not detectably on the NP stiffness parameter k, due to the finite size of the system. These finite size effects have been studied previously to

understand the concentration dependence of polymer nanocomposites, since varying the box size changes the effective NP concentration.[14] To make our analysis manageable, and to avoid unwarranted assumptions in the description of these finite size effects, we simply define $\tau_{far} \equiv \tau_\alpha(r = 10)$.

The interfacial relaxation time can evidently be either much larger or much smaller at different strengths of the NP–polymer interaction, which has been reported in earlier works for hard NPs.[13,27,45,46] We also see that $\tau_\alpha(r)/\tau_{far}$ increases with increasing k at strong interaction, while k has little impact on the segmental relaxation time when the NP–polymer interaction is weak. Upon cooling, the interfacial relaxation time increases for a weak
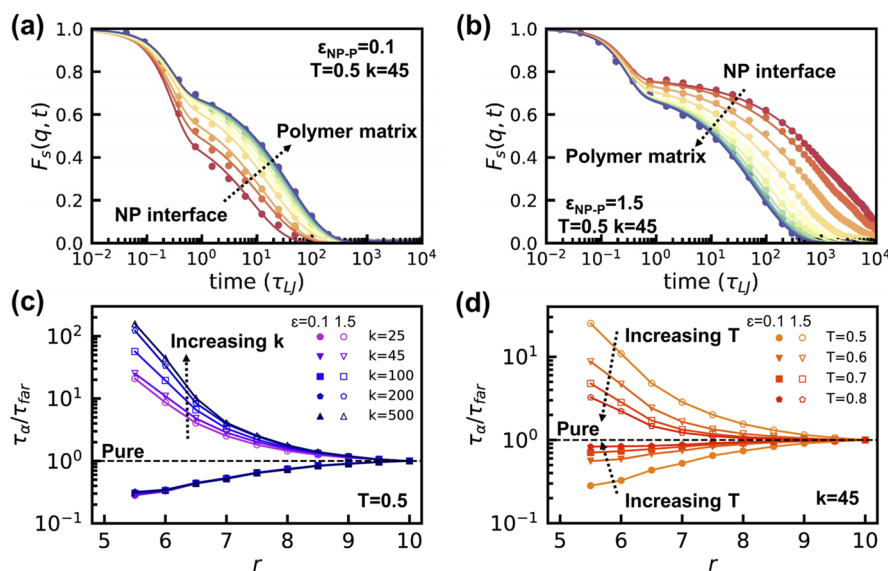
FIG. 2. Layer-resolved self-intermediate scattering function $F_s(q,t)$ at temperature $T = 0.5$ and variable NP stiffness $k = 45$ for systems having either (a) weakly $\varepsilon_{NP-P} = 0.1$ or (b) strongly $\varepsilon_{NP-P} = 1.5$ attractive interaction. Symbols are the collected data for each layer. Lines are the fit defined by Eq. (2) and adjacent layers are represented in coherent colors. The segmental relaxation near the NP is greatly accelerated for a weakly attractive interaction, while the NP with strongly attractive interaction slows down the dynamics. Relaxation time with (c) increasing k (5, 25, 45, 65, 100, 200, 500) at $T = 0.5$ and (d) increasing T (0.5, 0.6, 0.7, 0.8) at $k = 45$. $r = 5$ corresponds to the NP surface, and distance $r = 10$ is the neat polymer matrix. The interfacial relaxation time increases with increasing k or decreasing T at strong interaction. For a weak NP–polymer interaction strength, the interfacial polymer segmental relaxation time increases upon cooling and is nearly independent of k.

polymer–surface interaction, a trend that is also observed for the free interfacial layer mobility gradient of supported thin polymer films.[27,42–44] The $\tau_\alpha(r)/\tau_{far}$ ratio is always larger than 1 for a "strong" NP–polymer interaction strength (which slows down the dynamics at the interface) and lesser than 1 for a "weak" NP–polymer interaction strength (which accelerates the dynamics at the interface). The deviation between the segmental relaxation time near the interface and far-away polymer matrix generally becomes more pronounced at lower temperatures. In particular, for both weak and strong interactions, the ratio $\tau_\alpha(r)/\tau_{far}$ at small r deviates strongly from 1 at low T, but converges to a value near 1 at high T.

An insensitivity of the interfacial mobility layer to the NP–polymer interaction strength is also apparent in the work of Zhang et al. investigating nanocomposites with highly stiff NPs[26,27] and thin films with rigid walls.[47] This insensitivity of the mobile interfacial layer thickness to the boundary interaction stiffness and boundary rigidity seems to be robust, but recent work has shown that the mobile interfacial layer thickness near the solid substrate in supported polymer films depends strongly on the polymer topology.[48,49] The thickness of the mobile interfacial layer then seems to be predominantly a physical characteristic of the polymer matrix material.

### Stiffness dependence of dynamics of the interfacial region

We next discuss how a combination of temperature, NP–polymer interaction, and NP stiffness can influence the interfacial dynamics of the polymer surrounding the NP, both accelerating and slowing down the dynamics. It is already appreciated that varying the interfacial interaction strength can change the interfacial dynamics from faster than the surrounding polymer matrix (weak interfacial interactions) to slower than the polymer matrix (strong interfacial interactions). We show that the point at which this crossover occurs can be modulated by the NP stiffness parameter k. To emphasize this qualitative change in the interfacial mobility gradient, we focus on the *relative mobility change* in the interfacial layer, defined as the difference in the relaxation time between the innermost layer and the polymer matrix far from the NP, divided by the polymer matrix value. By denoting τ_α^{inter} as the relaxation time of the innermost layer, this "relative mobility change," $\delta\tau_\alpha = \frac{\tau_\alpha^{inter} - \tau_{far}}{\tau_{far}}$, increases with increasing k, and it has a stronger k dependence for a stronger NP–polymer

interaction, as shown in Fig. 3(a). Our observations are evidently qualitatively consistent with the experimental observations of Dadmun et al.,[33,35,36] in which faster polymer diffusion was observed with the addition of softer NPs. Direct quantitative comparison with these experiments is not possible because the mobility of the whole chain is not simply related to the polymer segmental dynamics.[28]

Figure 3 shows that $\delta\tau_\alpha$ can change sign for fixed moderate values of the interaction strength $\varepsilon_{NP-P} = (0.75, 0.5)$ and a fixed T when the NP stiffness is varied over a large range, while no sign change on $\delta\tau_\alpha$ is observed when ε_{NP-P} is relatively large or small. In Fig. 3(b), we further observe that if the NP stiffness is fixed to a moderate value, $k = 45$, and ε_{NP-P} is varied over a large range, $\delta\tau_\alpha$ changes sign near $\varepsilon_{NP-P} = 0.5$, regardless of T. This crossover in the interfacial dynamics was reported in a previous study of supported thin polymer films and polymer nanocomposites containing rigid NPs,[26,27,43,45] although this phenomenon was not emphasized in these prior works.

The softness dependence of the "crossover energy" ε_c at which $\delta\tau_\alpha$ changes sign is similar to the effect of rigidity on the binding transition between polymers in solution.[50,51] In Fig. 4(a), we see an increase in the segmental density profile near the NP interface when the pair energy ε_{NP-P} is increased. This change in the density profile passing through ε_c has been observed previously in supported polymer films,[41,44] and the density changes are similar to those expected for a polymer binding transition. Figure 4(b) provides evidence that the nanoparticles deform considerably when they are very soft, allowing the polymer segments to invade the average domain occupied by the NP, much like a polymer interpenetrating other polymers in the melt. This interpenetration phenomenon greatly complicates the interpretation of the spherically averaged density profiles and the observation of the density kink tentatively associated with the binding of the NP to the polymer matrix. Further details on the interfacial density gradient (Figs. S1 and S2) and polymer radius of gyration (Figs. S3 and S4) are discussed in the supplementary material. The NP shape change is also shown in Fig. S1(a). It was also observed that the sign of the T_g shift in thin supported films occurred for values of ε_{NP-P}, near where the density "kink" occurred near the supporting substrate.

The variation $\delta\tau_\alpha$ for the soft NPs has some features that are different from previous observations on supported films where a crossover value of the boundary stiffness parameter k_c was observed for fixed values of ε_{NP-P}.[44] We see that the effect of varying the NP stiffness on $\delta\tau_\alpha$ is likewise strong for a highly attractive interaction
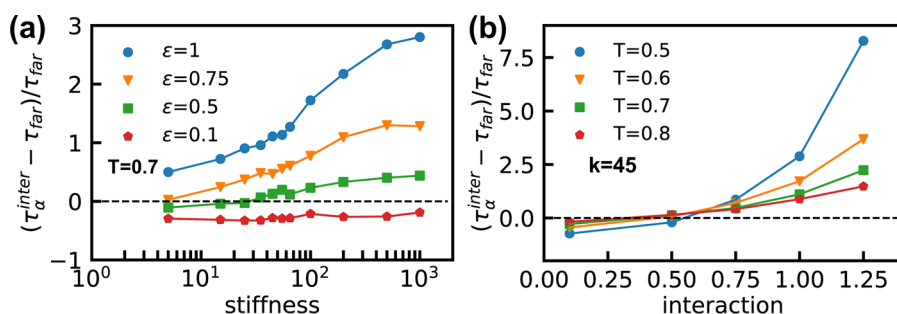
FIG. 3. Relative mobility change $\delta\tau_\alpha$ with (a) varying NP stiffness k at $T = 0.7$ and different ε_{NP-P} and (b) varying ε_{NP-P} at $k = 45$ and different T. There is a critical value of k at a fixed ε_{NP-P} and a critical value of ε_{NP-P} at a fixed k at which the dynamics at the interface switch from being faster to being slower than the bulk dynamics. Lines are a guide for the eye.
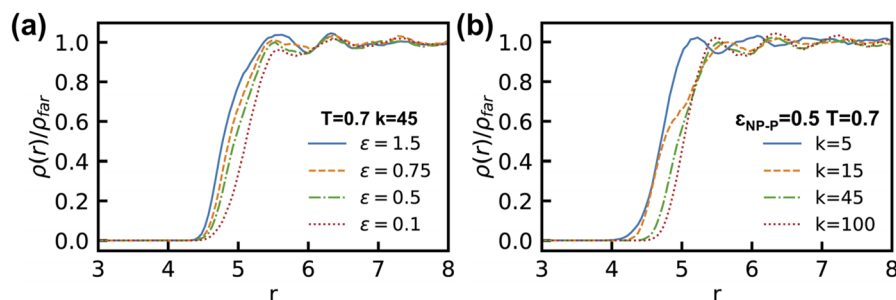
FIG. 4. Density profile for polymer chains with (a) varying ε_{NP-P} at $k = 45$ and $T = 0.7$ and (b) varying NP stiffness k at $T = 0.7$ and $\varepsilon_{NP-P} = 0.5$. r is the distance from the NP center. The icosahedral NP has radius of $r = 5$, while $r = 10$ is the neat polymer matrix.

between the NP and the polymer matrix. The magnitude of $\delta\tau_\alpha$ is generally positive, while there is virtually no variation of $\delta\tau_\alpha$ when the attractive interaction between the NP and the matrix is weak and is negative when the stiffness is varied over a large range. This unexpected trend in $\delta\tau_\alpha$ *is* attributed to the change in the shape of the NP as its stiffness is varied, which starts closer to the center of the softer NP, because more beads would be much closer to the center. The influence of the polymer–nanoparticle interaction strength on the dynamics of the outer layer of the NP is illustrated in Fig. S5 of the supplementary material. Changes in the segmental density profile near the NP surface and mobility gradient in the interfacial region are clearly more subtle for soft NPs because of the capacity of their interfaces to "crumple" in response to changes in ε_{NP-P}.

Based on the preceding discussion, we hypothesize that the crossover in the sign of the interfacial changes in the dynamics and the associated changes in the interfacial segmental density may be directly linked to a binding–unbinding transition between the NP and the polymer matrix.[52,53] The density changes near such a transition are much more subtle in polymer melts than in polymer solutions, where the binding transition signals a sharp change in the local density gradient near the boundary, whose location can have an appreciable temperature dependence. Interestingly, the effect of the substrate stiffness on the binding of polymers to surface transitions at low polymer concentration ("polymer adsorption") has apparently never been investigated either experimentally or by simulation before. We infer from recent simulation observations showing a strong effect of molecular rigidity on the strength of molecular binding[50,51] that boundary stiffness should likewise have an appreciable influence on the strength of molecular binding of isolated polymers in solution and polymer melts to substrates. Despite recent efforts to extend the binding–unbinding transition for polymer chains beyond the limits of the dilute regime,[52,53] the problem remains open, and this possibility of a binding transition underlying these changes in the interfacial density and dynamics deserves further study. A precise mapping of the dependence of ε_c on substrate stiffness, NP size, polymer segmental and topological structure, and temperature is a practically important problem, but this task is beyond the scope of the present work.

Effect of NP stiffness on the Debye–Waller factor, $\langle u^2 \rangle$

Along with the polymer segmental dynamics, we track the effect of NP stiffness on the picosecond caging dynamics associated with

the fast β-relaxation.[54] From the layer-resolved mean square displacement (MSD) of the beads of the polymer (modeling statistical segments of the polymer rather than atoms in our coarse-grained polymer model), we extract the "Debye–Waller parameter" $\langle u^2 \rangle$ as the value of the MSD at $t_{cage} = 1$ or a timescale of the order of 1 ps in laboratory units. This timescale corresponds to the typical order of magnitude of the β-relaxation time τ_β in atomic and molecular liquids.[55] In qualitative physical terms, $\langle u^2 \rangle$ quantifies the average "amplitude" of segmental motion arising from thermal agitation of the particles on a caging timescale. However, it should be noted that the magnitude of $\langle u^2 \rangle$ in cooled liquids is heavily weighted by relatively rare "mobile" particles on a ps timescale (a kind of dynamic heterogeneity) so that $\langle u^2 \rangle$ is not just a measure of the scale of "cage-rattling" around a mean position, as in crystals at low temperatures.[54] Figures 5(a) and 5(b) indicate the layer-resolved mean square displacement of the polymer statistical segments for a relatively weak and strong NP–polymer interaction strength, respectively. With a strong NP–polymer interaction, the mean amplitude of atomic motion near the inner layer (which can be taken as an inverse measure of local stiffness[56]), is diminished compared to segments far away from the NP boundary. In the weak interaction case, the interfacial dynamics is correspondingly accelerated. As in our discussion above of the relaxation time gradient near the surface of the NPs in Fig. 2, we see that the effect of the width of the gradient on $\langle u^2 \rangle$ is remarkably insensitive to both the NP rigidity and the NP–polymer interaction strength, while the magnitude of the change depends on these molecular variables.

We include a discussion of $\langle u^2 \rangle$ here because previous work has shown that this quantity can be highly predictive of the segmental relaxation in both bulk polymer,[57–60] metallic glass-forming and crystalline materials[61,62] and locally in the interfacial region of supported films.[49,63–65] The predictive power of this metric has become invaluable in the energy renormalization coarse-graining scheme developed for glass-forming systems.[66,67] The interfacial gradient of $\langle u^2 \rangle$ is also related to the variation of activation energies and local stiffness.[49] Figures 5(c) and 5(d) show the effect of varying NP stiffness, surface interaction, and temperature on $\langle u^2 \rangle$ as a function of the distance away from the center of the NPs. Evidently, the effect of the NP stiffness k is more pronounced when the polymer–surface interaction is strongly attractive, while the temperature effect is noticeable when the polymer–surface interaction is weakly attractive. The amplitude of the motion of the polymer segments in the interfacial region compared to the "bulk" fluid (corresponding to distances far away from the center of the isolated NP) is evidently
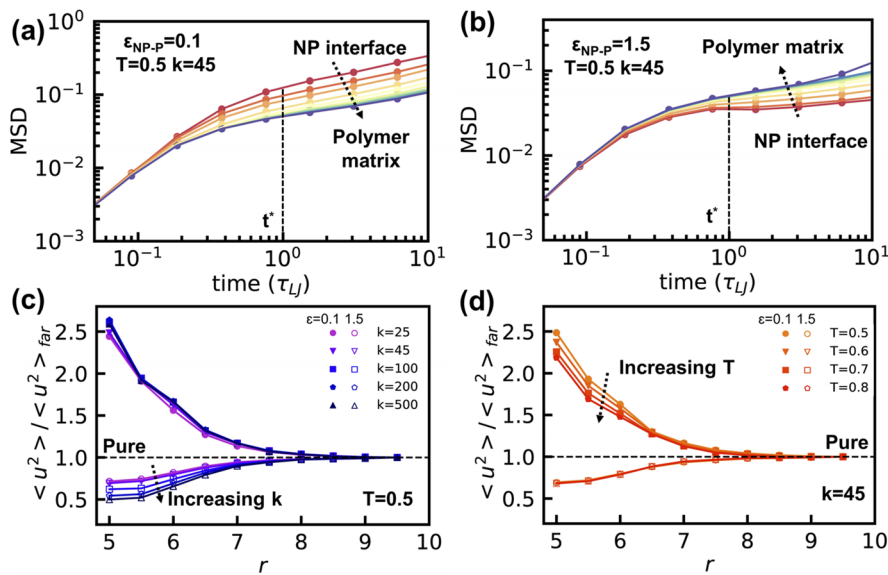
FIG. 5. Layer-resolved dynamics of polymer beads at (a) weak interaction and (b) strong interaction. Symbols are the collected data for each layer. Layers are shown in coherent colors. Radial averaged Debye–Waller factor $\langle u^2 \rangle$ for the polymer (c) with varying k at a fixed temperature $T = 0.5$ and (d) with varying T at a fixed $k = 45$ where r is the radial distance from the center of the NP and $\langle u^2 \rangle$ is the value of mean square displacement at $t = 1 = t_{cage}$.

larger when the NPs are stiffer. This trend is not obvious since we might have expected the structural relaxation time to monotonically increase as the segments become more localized in both the localization model[68] and the model of Leporini *et al.*[57,69] relating $\langle u^2 \rangle$ to the structural relaxation time τ_α determined from the intermediate scattering function. This counterintuitive trend can be understood from the fact that it is the value of $\langle u^2 \rangle$ relative to its value at a reference temperature or the value of $\langle u^2 \rangle$ at T_g (or similar reference temperature) that is important. Previous work on metallic glass alloys has shown that $\langle u^2(T) \rangle$ at the onset temperature T_A for non-Arrhenius relaxation correlates strongly with the fragility of glass-formation[61] and it is natural to expect T_A to depend on k. The quantification of this effect requires a systematic study of the relaxation time gradient and $\langle u^2 \rangle$ over a large range of T and this task is left for future work.

The difference between the mobility in the interfacial region from the bulk-like region far away from the NP surface generally becomes more pronounced at lower temperatures, although this difference becomes small at a characteristic value of the interaction strength ε_{NP-P} between the polymer matrix and the NP where the attractive and repulsive interactions nearly compensate. The interfacial dynamics compared to the bulk changes profoundly at this "critical" value of ε_{NP-P}, similar to a binding–unbinding transition.

CONCLUSION

This study investigates how the addition of deformable filler nanoparticles in polymer matrices compares with their hard NP counterparts, since the effect of NP stiffness on the structure and dynamics of polymer matrices has not been investigated from a molecular point of view in connection to glassy segmental dynamics. In particular, we simulate polymer nanocomposite systems with isolated model deformable NPs, and study the impact of NP stiffness, together with the NP–polymer interaction strength and tempera-

ture, on the interfacial polymer segmental dynamics. The polymer segmental relaxation becomes larger or smaller for relatively large or small polymer–surface interaction strengths, which we suggest may have its origin in a NP–polymer binding transition.[52,53] Increasing NP stiffness magnifies this effect and shifts the location of this crossover. However, such a crossover in segmental relaxation does not occur when temperature is varied as for polymers in solution.[70–75] Above or below the dynamical crossover, the segmental relaxation time can be much larger or smaller than its bulk value and essentially no gradient exists near the crossover point. A small change in the density profile near the surface can be seen above and below the crossover.[26,27] With stronger NP–polymer interaction, a densification of monomers at the interface correlates with lower mobility, while an opposite trend is observed with higher stiffness. We attribute this opposite trend to the change in shape of the NP, which is affected by the NP stiffness. Both the NP stiffness and the NP–polymer interaction can help to manipulate the dynamical crossover. The composition and chemical functionality of soft NP surfaces become then tunable parameters to control the interface dynamics and viscoelastic behavior of NP-filled polymer composites.

The picosecond caging dynamics of the polymer have also been tracked. The impact of the NP stiffness k on these dynamics is less pronounced at a weaker attractive interaction, while the effect of temperature is more pronounced. When the NPs are stiffer, the relative change of the picosecond motion compared to that at the far end of the polymer matrix from the NP is amplified with a stiffer NP. These results provide further evidence of general trends in the nanoscale glassy dynamics found before in thin films and in the interfcail regions of rigid nanoparticles, and offer a rational strategy for tuning the macroscopic thermomechanical properties of NP-filled polymer composites. Future studies with more realistic soft nanoparticles and in the regime of high NP-concentration will be important to bridge the gap between the nanoscale dynamics observed here and the emergent properties of the whole composite.

METHODS

In this work, we assumed a dilute dispersion of "soft" NPs in the polymer matrix. Our study of the dilute limit allows us to avoid interaction effects between NPs so that we may focus exclusively on the interfacial zone around the NPs. Following our previous studies,[13,27,46,76,77] we construct the PNC model with a single polyhedral NP under the periodic boundary conditions. Polymer chains are modeled using the Kremer–Grest spring-bead model,[78] with bonded monomers linked via a finitely extensive nonlinear elastic (FENE) potential with $R_0 = 1.5\,\sigma$ and the force constant $k_b = 30\,\varepsilon/\sigma_2$, where σ and ε are the parameters of the Lennard-Jones potential used for the non-bonded monomer–monomer interactions. Each chain has $N = 20$ monomers with mass m and diameter σ. The idealized NP consists of icosahedral shells using 356 Lennard-Jones (LJ) particles, corresponding to an inscribing sphere with radius of 5.0σ.[46] Each particle of the NP is tethered to its ideal equilibrium position by a spring force. We tune the NP stiffness via the spring constant k in a range of 5–1000. All the pairwise interactions in the system are the LJ potential with a cutoff at $r_C = 2.5\sigma \cdot \varepsilon_{ij}$ between monomers ε_{NP-P} and between NP particles ε_{NP-NP} being 1ε and 2ε, respectively, while the value between NP particles and monomers ε_{NP-P} is in the range of 0.1ε to 1.5ε. The size parameter between NP and monomer is $\sigma_{NP-P} = 1\sigma$.

All simulations are performed using the large-scale atomic/molecular massively parallel simulator (LAMMPS)[79] with standard LJ reduced units, where mass, length, temperature, and time are in units of m, σ, ε/k_B, and $\tau_{LJ} = \sigma\sqrt{m/\varepsilon}$, respectively. k_B is Boltzmann's constant. For a simple polymer like polystyrene (PS), our system can be loosely mapped to physical units[80] by taking $\sigma = 1$ nm, $\tau_{LJ} = 1$ ps and $\varepsilon = 7.7$ kJ/mol, leading to the glass transition temperature T_g close to 370 K. All simulations are conducted over a temperature range $0.5 \le T \le 0.8$ above T_g, which is in the range 0.3–0.4 for this model along an isobaric path at low pressure $P = 0.1$. A small value of pressure is chosen since atmospheric pressure is quite small. Using the mapping of LJ units described by Liu et al.[81] would yield $P \approx 2$ MPa. While this is larger than atmospheric pressure, the quantitative difference in our findings between this and $P = 0$ is small, and the qualitative conclusions are unaffected. We equilibrate systems using the isothermal–isobaric ensemble (NPT ensemble) for at least 3000 τ_{LJ}, from which the mean volume V is determined. We carry out data production runs using the volume determined from the equilibration step in the canonical ensemble (NVT ensemble) to avoid complications in the analysis introduced by a fluctuating simulation volume in an NPT ensemble. The equilibration time is extended in cases at low T and high ε_{NP-P}, such as, at $T = 0.5$, $\varepsilon_{NP-P} = 1.5$, which is considered as strongly attractive interaction, so that the system is equilibrated for at least 100 times the segmental relaxation time. In the slowest case, the equilibration time needed is 240 000 τ_{LJ}. The segmental dynamics are quantified using the self-intermediate scattering function

$$F_S(q,t) \equiv \frac{1}{N}\left\langle \sum_{j=1}^{N} e^{-i\boldsymbol{q}\cdot[r_j(t)-r_j(0)]} \right\rangle, \quad (1)$$

where $\boldsymbol{q}$ is the scattering vector, $\boldsymbol{r}_j$ is the position vector of polymer beads j, and N is the total number of polymer beads. To better describe the time dependence, we fit the simulation data of $F_s(q,t)$ within each shell to a phenomenological relaxation functional form[26]

$$F_S(q,t) = (1-A)e^{-(t/\tau_s)^{3/2}} + Ae^{-(t/\tau_\alpha)^\beta}, \quad (2)$$

where the vibrational relaxation time is assumed to be a constant $\tau_s = 0.29$ (of the order of 10^{-13} s in laboratory units). The characteristic segmental relaxation time τ_α can also be estimated as the time $F_S(q_0, t) = 0.2 \cdot q_0$ is the position of the first peak in the structure factor $S(q)$. The dependence of τ the fitting parameter A of Eq. (2) is discussed in Fig. S6 of the supplementary material. To quantify the dynamics gradient from the NP surface to polymer, we divided the outer space into shells with a fixed thickness 0.5 and compute F_S within each shell. The polymer beads are sorted into shells based on their location at time $t = 0$.

SUPPLEMENTARY MATERIAL

The effect of the nanoparticle stiffness on the density profile around the nanoparticle, the spatial variation of the polymer radius of gyration, the effect of varying stiffness parameter k on NP deformation, and the effect on the strength of the α relaxation are discussed in the supplementary material. This material is available free of charge at http://pubs.acs.org.

ACKNOWLEDGMENTS

AUTHOR DECLARATIONS

Conflict of Interest

The authors have no conflicts to disclose.

Author Contributions

Yuwen Zhu: Data curation (equal); Formal analysis (equal); Investigation (equal); Software (equal); Writing – original draft (equal); Writing – review & editing (equal). **Andrea Giuntoli**: Data curation (equal); Formal analysis (equal); Investigation (equal); Methodology (equal); Project administration (equal); Supervision (equal); Writing – original draft (equal); Writing – review & editing (equal). **Wengang Zhang**: Formal analysis (equal); Methodology (equal); Validation (equal); Writing – review & editing (equal). **Zhongqin Lin**: Funding acquisition (equal); Writing – review & editing (equal). **Sinan Keten**: Project administration (equal); Resources (equal); Supervision (equal); Writing – review & editing (equal). **Francis W. Starr**: Conceptualization (equal); Data curation (equal); Methodology (equal); Validation (equal); Writing – review & editing (equal). **Jack F. Douglas**: Conceptualization (equal); Formal analysis (equal); Methodology (equal); Supervision (equal); Validation

(equal); Writing – original draft (equal); Writing – review & editing (equal).

DATA AVAILABILITY

The data that support the findings of this study are available within the article and its supplementary material and from the corresponding authors upon reasonable request.

REFERENCES

[1] S. Fu, Z. Sun, P. Huang, Y. Li, and N. Hu, "Some basic aspects of polymer nanocomposites: A critical review," Nano Mater. Sci. **1**(1), 2–30 (2019).

[2] J. Jordan, K. I. Jacob, R. Tannenbaum, M. A. Sharaf, and I. Jasiuk, "Experimental trends in polymer nanocomposites—A review," Mater. Sci. Eng. A **393**(1–2), 1–11 (2005).

[3] F. Kundie, C. H. Azhari, A. Muchtar, and Z. A. Ahmad, "Effects of filler size on the mechanical properties of polymer-filled dental composites: A review of recent developments," J. Phys. Sci. **29**(1), 141–165 (2018).

[4] S. H. Ahn, S. H. Kim, B. C. Kim, K. B. Shim, and B. G. Cho, "Mechanical properties of silica nanoparticle reinforced poly(ethylene 2, 6-naphthalate)," Macromol. Res. **12**(3), 293–302 (2004).

[5] S. Yang, J. Choi, and M. Cho, "Elastic stiffness and filler size effect of covalently grafted nanosilica polyimide composites: Molecular dynamics study," ACS Appl. Mater. Interfaces **4**(9), 4792–4799 (2012).

[6] G. H. Lee, T. M. Choi, B. Kim, S. H. Han, J. M. Lee, and S.-H. Kim, "Chameleon-inspired mechanochromic photonic films composed of non-close-packed colloidal arrays," ACS Nano **11**(11), 11350–11357 (2017).

[7] T.-L. Lu and Y.-C. Tsai, "Sensitive electrochemical determination of acetaminophen in pharmaceutical formulations at multiwalled carbon nanotube-alumina-coated silica nanocomposite modified electrode," Sens. Actuators, B **153**(2), 439–444 (2011).

[8] J.-H. Liou, Z.-H. Wang, I.-H. Chen, S. S.-S. Wang, S.-C. How, and J.-S. Jan, "Catalase immobilized in polypeptide/silica nanocomposites via emulsion and biomineralization with improved activities," Int. J. Biol. Macromol. **159**, 931–940 (2020).

[9] J. Hyon, M. Gonzales, J. K. Streit, O. Fried, O. Lawal, Y. Jiao, L. F. Drummy, E. L. Thomas, and R. A. Vaia, "Projectile impact shock-induced deformation of one-component polymer nanocomposite thin films," ACS Nano **15**(2), 2439–2446 (2021).

[10] I.-Y. Jeon and J.-B. Baek, "Nanocomposites derived from polymers and inorganic nanoparticles," Materials **3**(6), 3654–3674 (2010).

[11] K. Müller, E. Bugnicourt, M. Latorre, M. Jorda, Y. Echegoyen Sanz, J. Lagaron, O. Miesbauer, A. Bianchin, S. Hankin, U. Bölz, G. Pérez, M. Jesdinszki, M. Lindner, Z. Scheuerer, S. Castelló, and M. Schmid, "Review on the processing and properties of polymer nanocomposites and nanocoatings and their applications in the packaging, automotive and solar energy fields," Nanomaterials **7**(4), 74 (2017).

[12] W. S. Junior, T. Emmler, C. Abetz, U. A. Handge, J. F. dos Santos, S. T. Amancio-Filho, and V. Abetz, "Friction spot welding of PMMA with PMMA/silica and PMMA/silica-g-PMMA nanocomposites functionalized via ATRP," Polymer **55**(20), 5146–5159 (2014).

[13] B. A. Pazmiño Betancourt, J. F. Douglas, and F. W. Starr, "Fragility and cooperative motion in a glass-forming polymer-nanoparticle composite," Soft Matter **9**(1), 241–254 (2013).

[14] F. W. Starr and J. F. Douglas, "Modifying fragility and collective motion in polymer melts with nanoparticles," Phys. Rev. Lett. **106**(11), 115702 (2011).

[15] H. Shin, K. Baek, J.-G. Han, and M. Cho, "Homogenization analysis of polymeric nanocomposites containing nanoparticulate clusters," Compos. Sci. Technol. **138**, 217–224 (2017).

[16] A. Bansal, H. Yang, C. Li, K. Cho, B. C. Benicewicz, S. K. Kumar, and L. S. Schadler, "Quantitative equivalence between polymer nanocomposites and thin polymer films," Nat. Mater. **4**(9), 693–698 (2005).

[17] P. Rittigstein, R. D. Priestley, L. J. Broadbelt, and J. M. Torkelson, "Model polymer nanocomposites provide an understanding of confinement effects in real nanocomposites," Nat. Mater. **6**(4), 278–282 (2007).

[18] T. Sasaki, T. Uchida, and K. Sakurai, "Effect of crosslink on the characteristic length of glass transition of network polymers," J. Polym. Sci., Part B: Polym. Phys. **44**(14), 1958–1966 (2006).

[19] S.-Y. Fu, X.-Q. Feng, B. Lauke, and Y.-W. Mai, "Effects of particle size, particle/matrix interface adhesion and particle loading on mechanical properties of particulate–polymer composites," Composites, Part B **39**(6), 933–961 (2008).

[20] A. S. Blivi, F. Benhui, J. Bai, D. Kondo, and F. Bédoui, "Experimental evidence of size effect in nano-reinforced polymers: Case of silica reinforced PMMA," Polym. Test. **56**, 337–343 (2016).

[21] S. Gam, J. S. Meth, S. G. Zane, C. Chi, B. A. Wood, K. I. Winey, N. Clarke, and R. J. Composto, "Polymer diffusion in a polymer nanocomposite: Effect of nanoparticle size and polydispersity," Soft Matter **8**(24), 6512 (2012).

[22] C.-Y. Teng, Y.-J. Sheng, and H.-K. Tsao, "Surface segregation and bulk aggregation in an athermal thin film of polymer-nanoparticle blends: Strategies of controlling phase behavior," Langmuir **33**(10), 2639–2645 (2017).

[23] Y. Fu, J. Michopoulos, and J.-H. Song, "Dynamics response of polyethylene polymer nanocomposites to shock wave loading," J. Polym. Sci., Part B: Polym. Phys. **53**(18), 1292–1302 (2015).

[24] J. J. Burgos-Mármol and A. Patti, "Unveiling the impact of nanoparticle size dispersity on the behavior of polymer nanocomposites," Polymer **113**, 92–104 (2017).

[25] A. Karatrantos, N. Clarke, R. J. Composto, and K. I. Winey, "Polymer conformations in polymer nanocomposites containing spherical nanoparticles," Soft Matter **11**(2), 382–388 (2015).

[26] W. Zhang, H. Emamy, F. Vargas-Lara, B. A. P. Betancourt, D. Meng, F. W. Starr, and J. F. Douglas, "The interfacial layers around nanoparticle and its impact on structural relaxation and glass transition in model polymer nanocomposites," in *Theory and Modeling of Polymer Nanocomposites* (Springer, 2021), pp. 101–131.

[27] W. Zhang, H. Emamy, B. A. Pazmiño Betancourt, F. Vargas-Lara, F. W. Starr, and J. F. Douglas, "The interfacial zone in thin polymer films and around nanoparticles in polymer nanocomposites," J. Chem. Phys. **151**(12), 124705 (2019).

[28] A. P. Holt, P. J. Griffin, V. Bocharova, A. L. Agapov, A. E. Imel, M. D. Dadmun, J. R. Sangoro, and A. P. Sokolov, "Dynamics at the polymer/nanoparticle interface in poly(2-vinylpyridine)/silica nanocomposites," Macromolecules **47**(5), 1837–1843 (2014).

[29] P. Bačová, F. Lo Verso, A. Arbe, J. Colmenero, J. A. Pomposo, and A. J. Moreno, "The role of the topological constraints in the chain dynamics in all-polymer nanocomposites," Macromolecules **50**(4), 1719–1731 (2017).

[30] M. H. Malakooti, M. R. Bockstaller, K. Matyjaszewski, and C. Majidi, "Liquid metal nanocomposites," Nanoscale Adv. **2**(7), 2668–2677 (2020).

[31] A. Tuteja, M. E. Mackay, C. J. Hawker, and B. Van Horn, "Effect of ideal, organic nanoparticles on the flow properties of linear polymers: Non-Einstein-like behavior," Macromolecules **38**(19), 8000–8011 (2005).

[32] A. Tuteja, M. E. Mackay, S. Narayanan, S. Asokan, and M. S. Wong, "Breakdown of the continuum Stokes–Einstein relation for nanoparticle diffusion," Nano Lett. **7**(5), 1276–1281 (2007).

[33] B. Miller, A. E. Imel, W. Holley, D. Baskaran, J. W. Mays, and M. D. Dadmun, "The role of nanoparticle rigidity on the diffusion of linear polystyrene in a polymer nanocomposite," Macromolecules **48**(22), 8369–8375 (2015).

[34] X.-M. Jia, R. Shi, G.-S. Jiao, T. Chen, H.-J. Qian, and Z.-Y. Lu, "Temperature effect on interfacial structure and dynamics properties in polymer/single-chain nanoparticle composite," Macromol. Chem. Phys. **218**(16), 1700029 (2017).

[35] S. Rostom and M. D. Dadmun, "The impact of nanoparticle softness on its tracer diffusion coefficient in all polymer nanocomposites," J. Appl. Phys. **127**(7), 074303 (2020).

[36] A. E. Imel, S. Rostom, W. Holley, D. Baskaran, J. W. Mays, and M. D. Dadmun, "The tracer diffusion coefficient of soft nanoparticles in a linear polymer matrix," RSC Adv. **7**(25), 15574–15581 (2017).

[37] T. Chen, H.-J. Qian, and Z.-Y. Lu, "Diffusion dynamics of nanoparticle and its coupling with polymers in polymer nanocomposites," Chem. Phys. Lett. **687**, 96–100 (2017).

[38] H. J. Martin, B. T. White, G. Yuan, T. Saito, and M. D. Dadmun, "Relative size of the polymer and nanoparticle controls polymer diffusion in all-polymer nanocomposites," Macromolecules **52**(7), 2843–2852 (2019).

[39] C. Chen, R. A. L. Wylie, D. Klinger, and L. A. Connal, "Shape control of soft nanoparticles and their assemblies," Chem. Mater. **29**(5), 1918–1945 (2017).

[40] E. Senses, M. Tyagi, M. Pasco, and A. Faraone, "Dynamics of architecturally engineered all-polymer nanocomposites," ACS Nano **12**(11), 10807–10816 (2018).

[41] W. Zhang, J. F. Douglas, and F. W. Starr, "Effects of a 'bound' substrate layer on the dynamics of supported polymer films," J. Chem. Phys. **147**(4), 044901 (2017).

[42] P. Z. Hanakata, J. F. Douglas, and F. W. Starr, "Local variation of fragility and glass transition temperature of ultra-thin supported polymer films," J. Chem. Phys. **137**(24), 244901 (2012).

[43] P. Z. Hanakata, J. F. Douglas, and F. W. Starr, "Interfacial mobility scale determines the scale of collective motion and relaxation rate in polymer films," Nat. Commun. **5**, 4163 (2014).

[44] P. Z. Hanakata, B. A. Pazmiño Betancourt, J. F. Douglas, and F. W. Starr, "A unifying framework to quantify the effects of substrate interactions, stiffness, and roughness on the dynamics of thin supported polymer films," J. Chem. Phys. **142**(23), 234907 (2015).

[45] F. W. Starr, J. F. Douglas, D. Meng, and S. K. Kumar, "Bound layers 'cloak' nanoparticles in strongly interacting polymer nanocomposites," ACS Nano **10**(12), 10960–10965 (2016).

[46] F. W. Starr, T. B. Schrøder, and S. C. Glotzer, "Molecular dynamics simulation of a polymer melt with a nanoscopic particle," Macromolecules **35**(11), 4481–4492 (2002).

[47] W. Xia, S. Mishra, and S. Keten, "Substrate vs. free surface: Competing effects on the glass transition of polymer thin films," Polymer **54**(21), 5942–5951 (2013).

[48] W. Zhang, J. F. Douglas, A. Chremos, and F. W. Starr, "Structure and dynamics of star polymer films from coarse-grained molecular simulations," Macromolecules **54**(12), 5344–5353 (2021).

[49] W. Zhang, F. W. Starr, and J. F. Douglas, "Activation free energy gradient controls interfacial mobility gradient in thin polymer films," J. Chem. Phys. **155**(17), 174901 (2021).

[50] C. Forrey, J. F. Douglas, and M. K. Gilson, "The fundamental role of flexibility on the strength of molecular binding," Soft Matter **8**(23), 6385–6392 (2012).

[51] F. Vargas-Lara, F. W. Starr, and J. F. Douglas, "Molecular rigidity and enthalpy-entropy compensation in DNA melting," Soft Matter **13**(44), 8309–8330 (2017).

[52] J. Dudowicz, J. F. Douglas, and K. F. Freed, "Lattice theory for binding of linear polymers to a solid substrate from polymer melts: I. Influence of chain connectivity on molecular binding and adsorption," J. Chem. Phys. **151**(12), 124706 (2019).

[53] J. Dudowicz, J. F. Douglas, and K. F. Freed, "Lattice theory for binding of linear polymers to a solid substrate from polymer melts. II. Influence of van der Waals interactions and chain semiflexibility on molecular binding and adsorption," J. Chem. Phys. **151**(12), 124709 (2019).

[54] B. A. Pazmiño Betancourt, F. W. Starr, and J. F. Douglas, "String-like collective motion in the α- and β-relaxation of a coarse-grained polymer melt," J. Chem. Phys. **148**(10), 104508 (2018).

[55] V. N. Novikov, "Vibration anharmonicity and fast relaxation in the region of the glass transition," Phys. Rev. B **58**(13), 8367–8378 (1998).

[56] B. R. Frieberg, E. Glynos, G. Sakellariou, M. Tyagi, and P. F. Green, "Effect of molecular stiffness on the physical aging of polymers," Macromolecules **53**(18), 7684–7690 (2020).

[57] L. Larini, A. Ottochian, C. De Michele, and D. Leporini, "Universal scaling between structural relaxation and vibrational dynamics in glass-forming liquids and polymers," Nat. Phys. **4**(1), 42–45 (2007).

[58] B. A. Pazmiño Betancourt, P. Z. Hanakata, F. W. Starr, and J. F. Douglas, "Quantitative relations between cooperative motion, emergent elasticity, and free volume in model glass-forming polymer materials," Proc. Natl. Acad. Sci. U. S. A. **112**(10), 2966–2971 (2015).

[59] F. Puosi, A. Tripodo, M. Malvaldi, and D. Leporini, "Johari–Goldstein heterogeneous dynamics in a model polymer," Macromolecules **54**(5), 2053–2058 (2021).

[60] A. Tripodo, F. Puosi, M. Malvaldi, S. Capaccioli, and D. Leporini, "Coincident correlation between vibrational dynamics and primary relaxation of polymers with strong or weak Johari-Goldstein relaxation," Polymers **12**(4), 761 (2020).

[61] J. F. Douglas, B. A. Pazmino Betancourt, X. Tong, and H. Zhang, "Localization model description of diffusion and structural relaxation in glass-forming Cu–Zr alloys," J. Stat. Mech.: Theory Exp. **2016**(5), 054048.

[62] H. Zhang, X. Wang, and J. F. Douglas, "Localization model description of diffusion and structural relaxation in superionic crystalline UO_2," J. Chem. Phys. **151**(7), 071101 (2019).

[63] M. Becchi, A. Giuntoli, and D. Leporini, "Molecular layers in thin supported films exhibit the same scaling as the bulk between slow relaxation and vibrational dynamics," Soft Matter **14**(43), 8814–8820 (2018).

[64] G. Mahmud, H. Zhang, and J. F. Douglas, "Localization model description of the interfacial dynamics of crystalline Cu and $Cu_{64}Zr_{36}$ metallic glass films," J. Chem. Phys. **153**(12), 124508 (2020).

[65] G. Mahmud, H. Zhang, and J. F. Douglas, "Localization model description of the interfacial dynamics of crystalline Cu and $Cu_{64}Zr_{36}$ metallic glass nanoparticles," Eur. Phys. J. E **44**(3), 33 (2021).

[66] W. Xia, J. Song, N. K. Hansoge, F. R. Phelan, Jr., S. Keten, and J. F. Douglas, "Energy renormalization for coarse-graining the dynamics of a model glass-forming liquid," J. Phys. Chem. B **122**(6), 2040–2045 (2018).

[67] W. Xia, N. K. Hansoge, W. S. Xu, F. R. Phelan, S. Keten, and J. F. Douglas, "Energy renormalization for coarse-graining polymers having different segmental structures," Sci. Adv. **5**(4), eaav4683 (2019).

[68] D. S. Simmons, M. T. Cicerone, Q. Zhong, M. Tyagi, and J. F. Douglas, "Generalized localization model of relaxation in glass-forming liquids," Soft Matter **8**(45), 11455–11461 (2012).

[69] S. Bernini, F. Puosi, and D. Leporini, "Cage rattling does not correlate with the local geometry in molecular liquids," J. Non-Cryst. Solids **407**, 29–33 (2015).

[70] J. F. Douglas, A. M. Nemirovsky, and K. F. Freed, "Polymer-polymer and polymer-surface excluded volume effects in flexible polymers attached to an interface: Comparison of renormalization group calculations with Monte Carlo and direct enumeration data," Macromolecules **19**(7), 2041–2054 (1986).

[71] J. F. Douglas, S. Q. Wang, and K. F. Freed, "Test of renormalization group crossover dependence: Comparison with exact solution for a polymer attached to a penetrable interacting hypersurface," Macromolecules **19**(8), 2207–2220 (1986).

[72] J. F. Douglas, S. Q. Wang, and K. F. Freed, "Flexible polymers with excluded volume at a penetrable interacting surface," Macromolecules **20**(3), 543–551 (1987).

[73] J. F. Douglas, "Surface-interacting polymers: An integral-equation and fractional-calculus approach," Macromolecules **22**(4), 1786–1797 (1989).

[74] M. Adamuti-Trache, W. E. McMullen, and J. F. Douglas, "Segmental concentration profiles of end-tethered polymers with excluded-volume and surface interactions," J. Chem. Phys. **105**(11), 4798–4811 (1996).

[75] J. F. Douglas and K. F. Freed, "Modification of continuum chain model of surface-interacting polymers to describe the crossover between weak and strong adsorption," Macromolecules **30**(6), 1813–1817 (1997).

[76] F. W. Starr, T. B. Schrøder, and S. C. Glotzer, "Effects of a nanoscopic filler on the structure and dynamics of a simulated polymer melt and the relationship to ultrathin films," Phys. Rev. E **64**(2), 021802 (2001).

[77] H. Emamy, S. K. Kumar, and F. W. Starr, "Diminishing interfacial effects with decreasing nanoparticle size in polymer-nanoparticle composites," Phys. Rev. Lett. **121**(20), 207801 (2018).

[78] G. S. Grest and K. Kremer, "Molecular dynamics simulation for polymers in the presence of a heat bath," Phys. Rev. A **33**(5), 3628–3631 (1986).

[79] S. Plimpton, *Fast Parallel Algorithms for Short-Range Molecular Dynamics* (Sandia National Laboratories, Albuquerque, NM, 1993).

[80] J.-L. Barrat, J. Baschnagel, and A. Lyulin, "Molecular dynamics simulations of glassy polymers," Soft Matter **6**(15), 3430 (2010).

[81] A. Y. Liu, H. Emamy, J. F. Douglas, and F. W. Starr, "Effects of chain length on the structure and dynamics of semidilute nanoparticle–polymer composites," Macromolecules **54**(7), 3041–3051 (2021).